# Ultrasonic spectrum in Fibonacci acoustic superlattices

Yong-yuan Zhu and Nai-ben Ming*

*Laboratory of Solid State Microstructures, Nanjing University, People's Republic of China*

Wen-hua Jiang

*Institute of Acoustics, Nanjing University, People's Republic of China*

A new type of superlattice, a Fibonacci acoustic superlattice, is presented. Its ultrasonic spectrum, which is excited by the piezoelectric effect, has been studied theoretically and experimentally. The results are in good agreement with each other.

The discovery of quasicrystalline phases in metallic alloys[1] has opened a new field in solid-state physics. Since then, a lot of work has been done on the vibrational properties of the one-dimensional quasiperiodic superlattice, a heterostructure with quasiperiodic ordering of multilayers.[2-6] The spectra observed were those of thermally excited phonons and the superlattices are made from materials such as GaAs-AlAs, Nb-Cu, etc. with their modulated wavelength of several nanometers comparable with the wavelength of a de Broglie wave. However, there exists another type of superlattice. It is made from a piezoelectric single crystal and its modulated wavelength is in the range of several micrometers to tens of micrometers, which is comparable with the wavelengths of ultrasonic waves. We are interested in the ultrasonic spectrum excited by the piezoelectric effect which have extensive applications in acoustic devices. In our previous work,[7,8] we investigated the ultrasonic excitation by the piezoelectric effect in a periodic superlattice of a single crystal of $LiNbO_3$ with periodic laminar ferroelectric-domain structures. On that basis, we have studied theoretically, in this paper, the ultrasonic spectrum excited by a Fibonacci superlattice made from $LiNbO_3$ crystals. We have also verified quantitatively the self-similar structures of the ultrasonic spectrum experimentally. A good agreement with the theory is obtained.

The piezoelectric acoustic superlattice can be viewed as a structure composed of a series of sound $\delta$ sources arranged periodically or quasiperiodically. These $\delta$ sources are generated by the discontinuity of the piezoelectric stress which is the product of a piezoelectric coefficient and electric field. So, there are two ways to prepare a periodic or quasiperiodic acoustic superlattice. The first one is to use piezoelectric crystals such as a $LiNbO_3$ single crystal with periodic or quasiperiodic laminar ferroelectric-domain structures induced by the growth striations (Figs. 1 and 2).[9-12] The sign of a piezoelectric coefficient of the layered crystal changes alternately. In this case, the piezoelectric coefficient is discontinuous at the ferroelectric-domain boundaries which become sound sources under the action of an alternating external electric field and the excited acoustic waves are bulk waves. The second one is to fabricate an interdigital surface-

wave transducer with electrode intervals varying periodically or quasiperiodically (Figs. 3 and 4). The transducers are easily fabricated by a standard photolithographic technique.[13,14] Aluminum electrodes are deposited on a piezoelectric substrate such as a single-domain crystal of $LiNbO_3$. When an alternating external voltage is applied onto the electrodes, an electric field is built beneath the surface of the substrate as shown in Figs. 3(b) and 4(b), which can be simplified to Figs. 3(c) and 4(c).[15] The electric field generated beneath the surface of the substrate alternates its sign periodically or quasiperiodically. In this case, the electric field is discontinuous on the bisect line of each electrode beneath the surface of the substrate which is also a sound source and the excited acoustic waves are surface waves.

In both cases, the physical mechanism of ultrasonic excitation is obvious. According to Bömmel and Dransfeld,[16] under the action of an external electric field,
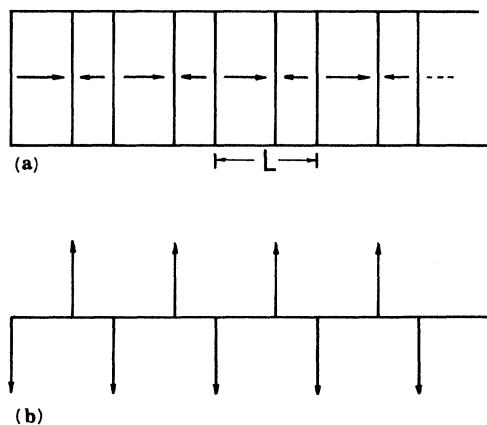


FIG. 1. Acoustic superlattice of $LiNbO_3$ crystals with periodic ferroelectric-domain structures. (a) Schematic diagram of periodic acoustic superlattice with the periodicity of $L$ (the arrows indicate the directions of the spontaneous polarization). (b) Corresponding sound $\delta$ sources.
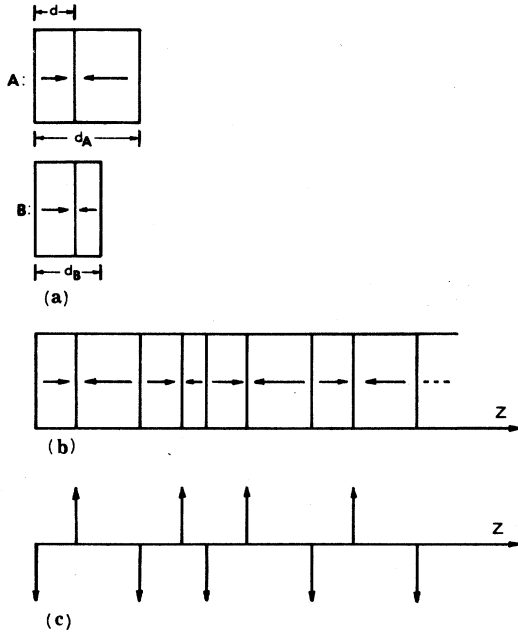
(a)

(b)

(c)

FIG. 2. Fibonacci acoustic superlattice of $LiNbO_3$ crystals. (a) The two blocks of a Fibonacci acoustic superlattice, each composed of one positive and one negative ferroelectric domain. (b) Schematic diagram of a Fibonacci acoustic superlattice (the arrows indicate the directions of the spontaneous polarization). (c) Corresponding sound $\delta$ sources.

the discontinuity in piezoelectric stress at the ferroelectric-domain boundaries (or on the bisect line of each electrode beneath the surface of the substrate) must be balanced by a strain $S(u_m)$. Here $u_m$ represents the position where the discontinuity takes place. This strain will propagate as a wave

$$S(u) = S(u_m)\cos(wt - ku) . \tag{1}$$

So each domain boundary (or the bisect line of each electrode where the discontinuity of electric field takes place) can be viewed as a sound $\delta$ source [see Figs. 1(b), 2(c), 3(d), and 4(d)].

Because of this similarity, in what follows we will limit ourselves to $LiNbO_3$ crystals with quasiperiodic laminar ferroelectric-domain structures. The results obtained will suit each other.

The Fibonacci acoustic superlattice of a $LiNbO_3$ crystal consists of two fundamental blocks of $A$ and $B$. The widths of these two blocks are different, each composed of one positive and one negative ferroelectric domain as shown in Fig. 2(a). The quasiperiodicity can be realized with a Fibonacci sequence of blocks $A$ and $B$ fulfilling relations:[17]

$$S(1) = |A|, \quad S(2) = |AB|, \quad S(3) = |AB:A| ,$$
$$S(4) = |ABA:AB|, \quad S(n) = |S(n-1):S(n-2)| , \tag{2}$$

and the ratio of the thicknesses of $A,B$ blocks just equals the golden mean, i.e.,

$$d_A/d_B = \tau = (1 + \sqrt{5})/2 . \tag{3}$$

The Fibonacci acoustic superlattice thus obtained is shown in Fig. 2(b).

We assume that the lateral dimensions of the Fibonacci acoustic superlattice are much larger than the width of the ferroelectric domains and that the normal of the domain boundaries coincides with the $z$ axis; then the one-dimensional model is applicable. Under these conditions, when an alternating voltage applied on the $\{0001\}$ faces of the sample, a longitudinal planar wave propagating along the $z$ axis will be excited inside the superlattice. It obeys the wave equation

$$\partial^2 u_3/\partial z^2 - (1/v^2)\partial^2 u_3/\partial t^2$$
$$= (2h_{33}D_3/C_{33}^D)\sum_m (-1)^m \delta(z - z_m) , \tag{4}$$

where $u_3$ represents the particle displacemnt in the $z$ direction, $v$ is the sound velocity, $h_{33}$, $C_{33}^D$, and $D_3$ are the piezoelectric, elastic coefficients, and electric displacement, respectively. $\{z_m\}$ are the positions of the

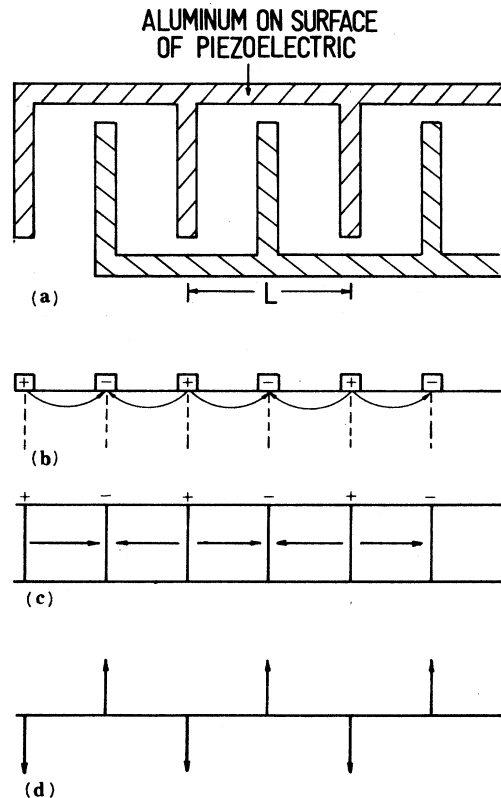

ALUMINUM ON SURFACE
OF PIEZOELECTRIC

(a)

(b)

(c)

(d)

FIG. 3. (a) Periodic interdigital transducer schematic diagram with the periodicity of $L$. (b) and (c) are side views of the interdigital transducer, showing electric field patterns inside the thin skin of the substrate. (b) Actual electric field pattern. (c) Simplified electric field pattern. (d) Corresponding sound $\delta$ sources.

ferroelectric-domain boundaries.

Equation (4) is a fundamental wave equation governing the excitation and propagation of sound waves in a piezoelectric superlattice. The term on the right-hand side stands for the exciting source of the sound wave. As above mentioned, the ultrasonic waves in such a superlattice are excited by a series of $\delta$ sources at the domain boundaries, which is also shown in Eq. (4). Therefore, we can make use of the impulse response model[13,14] to obtain the ultrasonic spectrum excited by the Fibonacci acoustic superlattice of LiNbO$_3$ crystals.

As can be seen in Fig. 2(c), the $\delta$ sources can be divided into two parts, one for positive $\delta$ sources, the other for negative $\delta$ sources. Each forms a Fibonacci sequence. The negative is displaced a distance $d$ relative to the positive. Performing Fourier transforms on the positive terms and the negative terms on the right-hand side of Eq. (4) separately, and adding them together, we can get the ultrasonic spectrum for an infinite array, which is

$$H(k) \propto \sin(kd/2) \sum_{m,n} (\sin X_{m,n}/X_{m,n})$$

$$\times \delta(k - 2\pi(m + n\tau)/D), \quad (5)$$

where $X_{m,n} = \pi\tau(m\tau - n)/(1+\tau^2)$, $D = \tau d_A + d_B$, and $k$ is the wave vector. In deriving Eq. (5), the projection method has been used.[18,19] The appearance of the term $\sin(kd/2)$ is due to the relative displacement between the



(a)        FREQUENCY(MHz)



(b)  ↑         ↑              ↑                    ↑
    (1 0)   (0 1)          (1 1)                (1 2)



(c)       ↑              ↑                    ↑
        (0 1)          (1 1)                (1 2)

FIG. 5. Ultrasonic spectrum for an eighth-generation Fibonacci acoustic superlattice. (a) Ultrasonic spectrum calculated for a LiNbO$_3$ crystal. $R$, relative value of radiation resistance. (b) Ultrasonic spectrum measured. (c) The same as (b) with the amplitude magnified. In both (b) and (c) the amplitude is in logarithmic scale.

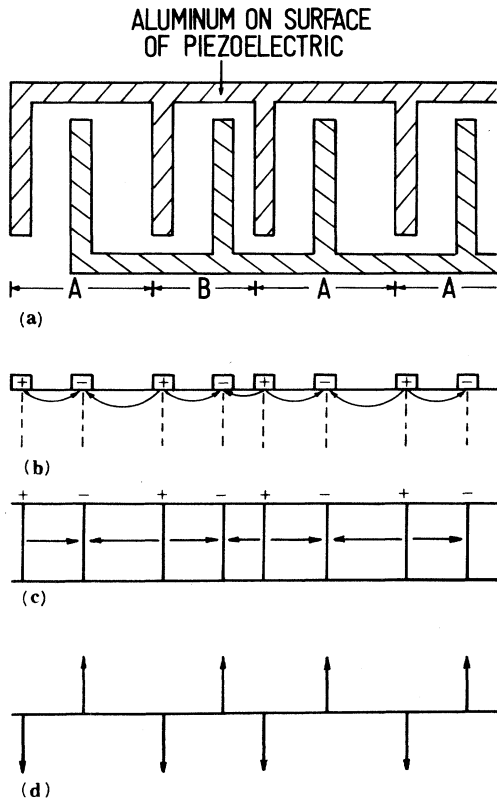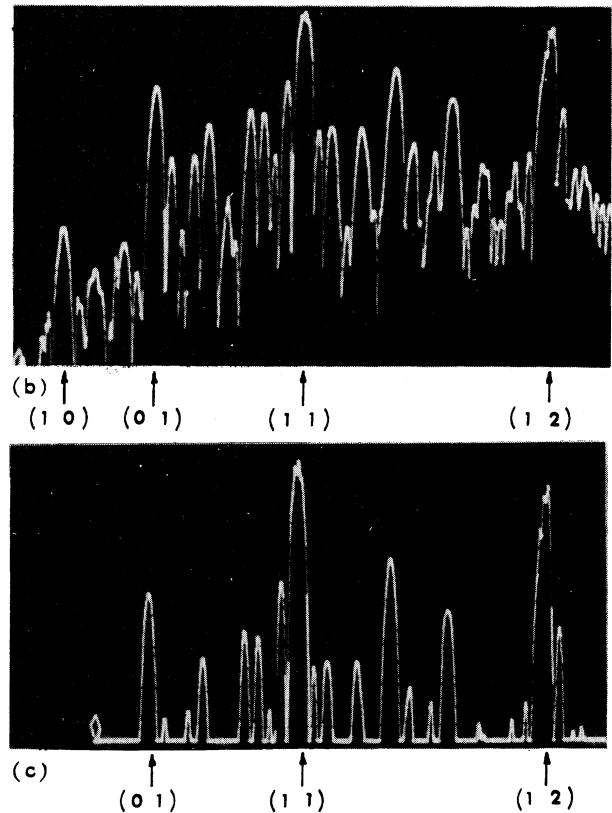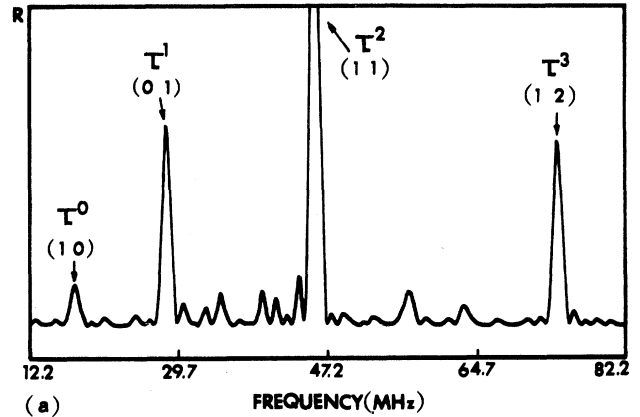ALUMINUM ON SURFACE
OF PIEZOELECTRIC



FIG. 4. (a) Quasiperiodic interdigital transducer schematic diagram. (b) and (c) are side views of the interdigital transducer, showing electric field patterns inside the thin skin of the substrate. (b) Actual electric field pattern. (c) Simplified electric field pattern. (d) Corresponding sound $\delta$ sources.

positions of positive $\delta$ sources and that of negative $\delta$ sources. The resonant peaks in the ultrasonic spectrum can be obtained from the $\delta$ functions in Eq. (5), which is $k = 2\pi(m + n\tau)/D$, or

$$f_{m,n} = v(m + n\tau)/D , \tag{6}$$

where $m, n$ are integers. The most significant resonant peaks in ultrasonic spectrum occur at $f = f_{m,n}$ for which $X_{m,n}$ is small. This means that $n/m$ must be close to $\tau$. It is well known that the best rational approximants to $\tau$ occur when $m$ and $n$ are successive Fibonacci integers,[20] $(m,n) = (F_{p-1}, F_p)$, where $F_{p+1} = F_p + F_{p-1}$ and $(F_0, F_1) = (0,1)$. For these values of $(m,n)$, $f_{m,n}$ takes the form of (integer)$v\tau^p/D$ and these resonant peaks are labeled $\tau^p$.

The results are much similar to that of acoustic-phonon transmission[5] except for the substitution of $f_{m,n} = v(m + n\tau)/D$ for $f_{m,n} = v(m + n\tau)/2D$ and of peaks for dips. These can be explained as follows. In the case of excitation of ultrasonic waves, if the piezoelectric medium is a superlattice one, the ultrasonic waves will be excited on the ferroelectric-domain boundaries. The waves coming from successive boundaries will interfere with each other. Those satisfying the constructive interference will appear as resonant peaks in the ultrasonic spectrum. Whereas in the case of acoustic-phonon transmission when the phonons, reflected from successive interfaces satisfy the constructive interference, they will appear as dips in transmission spectrum. Obviously, the peaks in the former case just correspond to the dips in the latter case. The occurrence of the factor $\frac{1}{2}$ in the expression for dip frequencies is due to the fact that the path difference between phonons reflected from the adjacent interfaces is twice as large as the path difference between the ultrasonic waves excited on the adjacent ferroelectric-domain boundaries.

We have calculated the ultrasonic spectrum excited by the Fibonacci acoustic superlattice numerically. In order to be compared with the experiments only the ultrasonic spectrum of the superlattice of the eighth Fibonacci generation has been shown in Fig. 5(a), with the parameters selected to be in line with the experiments. It is worth noting that the resonant peaks obey Eq. (6). In this figure, several frequencies predicted by the expression $f = f_{m,n} = (m,n)$ are indicated by arrows. As expected, the main peaks are observed at $f_{m,n}$ for which $m$ and $n$ are neighboring Fibonacci numbers, as indicated by $\tau^p$.

Detailed calculations have shown that the resonant peaks densely fill reciprocal space in a self-similar manner. It is just expected. It is well known that the self-similarity exists in the spectra of phonon,[2-6] electron energy,[4] polariton,[21] and in x-ray diffraction,[17] etc. Here again, in the ultrasonic spectrum excited by the Fibonacci acoustic superlattice of LiNbO$_3$ crystals, the self-similarity also exists. It may be said that the self-similarity is a common feature of the Fibonacci superlattices and is a reflection of the self-similar structure of Fibonacci superlattices in reciprocal space.

Experimentally, we have fabricated several quasi-periodic surface-wave interdigital transducers of the eighth Fibonacci generation. Aluminum electrodes are deposited on the surface of a single-domain crystal of LiNbO$_3$. The intervals between the electrodes varied successively according to the Fibonacci sequence. In this case, the surface-wave velocity $v = 3944$ m/sec. The oth-
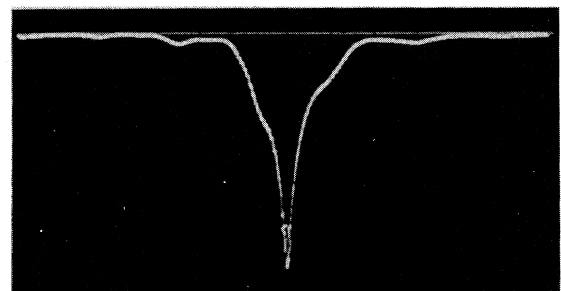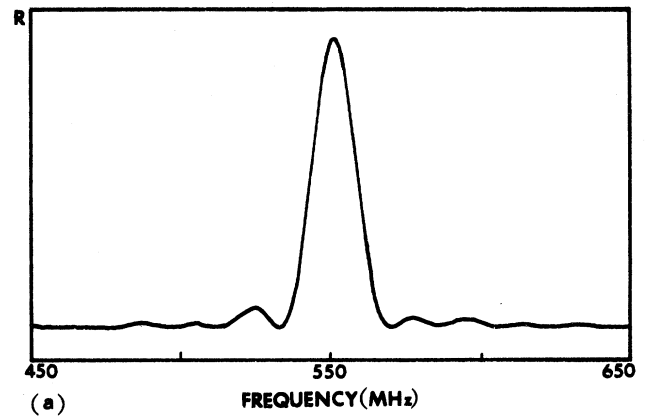


R

450                    550                 650

(a)           FREQUENCY(MHz)



(b)

FIG. 6. Ultrasonic spectrum for a periodic acoustic superlattice of a LiNbO$_3$ crystal. (a) Ultrasonic spectrum calculated. $R$, relative value of radiation resistance. (b) Measured magnitude of the reflection coefficient. The horizontal scale is frequency centered at 550 MHz with a scan width $f = 200$ MHz.

TABLE I. Comparison between resonance frequencies calculated and measured for a quasiperiodic surface-wave interdigital transducer.

| Vibrational mode | Resonance frequency | $f$ (MHz) |
|---|---|---|
| $(m,n)$ | calc. | meas. |
| (1,0) | 17.5 | 17.5 |
| (0,1) | 28.3 | 28.4 |
| (1,1) | 45.8 | 45.8 |
| (1,2) | 74.1 | 74.5 |

er parameters are $d = 39.0$ $\mu$m, $d_B = 62.3$ $\mu$m, and $d_A = 100.8$ $\mu$m which were measured by an optical microscope. The ultrasonic spectra are measured, which is the ratio of output voltage to input voltage. In the measurement, the frequency scan range of the frequency spectrum analyzer is selected to be from 12.2 to 82.2 MHz. The output voltage signals which satisfy the resonant conditions, i.e., $f_{m,n} = V(m + n\tau)/D$, are strengthened. The others are diminished. Figures 5(b) and 5(c) show one of these results. In the ultrasonic spectrum many sharp peaks appear at nonequal intervals. It is clear that there exists a one to one correspondence between the resonant peaks in Figs. 5(a) and 5(b) or 5(c). Table I shows the results calculated and measured. The agreement is quite satisfactory.

In order to compare the ultrasonic spectrum of the Fibonacci acoustic superlattice with that of the periodic acoustic superlattice, Figs. 6(a) and 6(b) show the theoretical and the experimental ultrasonic spectra obtained from a periodic acoustic superlattice of a LiNbO$_3$ crystal with periodic laminar ferroelectric-domain structures.

The analysis and the experiment are analogous to our previous work.[7,8] The resonant frequency measured is 555 MHz, close to the theoretical one, 553 MHz, which is calculated from $f = v/L$ with $L = 13.2$ $\mu$m and $v = 7300$ m/sec. Here $L$ is the periodicity of the periodic acoustic superlattice. Obviously Figs. 5 and 6 bear no resemblance to each other.

In conclusion, we have studied and obtained some of the features of the ultrasonic spectrum excited by a Fibonacci acoustic superlattice. Two ways to fabricate such a superlattice are presented. The superlattice is different from the traditional one in that it is a piezoelectric single crystal and the modulated wavelength is much larger. The ultrasonic spectrum is excited by the piezoelectric effect. The theoretical results are quantitatively verified by the experiments.

---

[*]To whom all communications regarding this paper should be addressed.

[1]D. Schechtman, I. Blech, D. Gratias, and J. W. Cahn, Phys. Rev. Lett. 53, 1951 (1984).

[2]J. P. Lu, T. Odagaki, and J. L. Birman, Phys. Rev. B 33, 4809 (1986).

[3]M. Kohmoto and J. R. Banavar, Phys. Rev. B 34, 563 (1986).

[4]F. Nori and J. P. Rodriguez, Phys. Rev. B 34, 2207 (1986).

[5]S. Tamura and J. P. Wolfe, Phys. Rev. B 36, 3491 (1987).

[6]X. K. Zhang, H. Xia, G. X. Cheng, A. Hu, and D. Feng, Phys. Lett. A 136, 312 (1989).

[7]Y. Y. Zhu, N. B. Ming, W. H. Jiang, and Y. A. Shui, Appl. Phys. Lett. 53, 1381 (1988).

[8]Y. Y. Zhu, N. B. Ming, W. H. Jiang, and Y. A. Shui, Appl. Phys. Lett. 53, 2278 (1988).

[9]N. B. Ming, J. F. Hong, and D. Feng, J. Mater. Sci. 27, 1663 (1982).

[10]N. B. Ming, J. F. Hong, Z. M. Sung, and Y. S. Yang, Acta Phys. Sin. (in Chinese) 30, 1672 (1981).

[11]J. F. Hong and Y. S. Yang, Acta Opt. Sin. (in Chinese) 4, 821 (1986).

[12]A. Feisst and P. Koidl, Appl. Phys. Lett. 47, 1125 (1985).

[13]R. H. Tancrel and M. G. Holland, Proc. IEEE 59, 395 (1971).

[14]C. S. Hartmann, D. T. Bell, Jr., and R. C. Rosenfeld, IEEE Trans. Sonics Ultrason. 20, 80 (1973).

[15]W. R. Smith, H. M. Gerard, J. H. Collins, T. M. Reeder, and H. J. Shaw, IEEE Trans. Microwave Theory Tech. 17, 856 (1969).

[16]H. E. Bömmel and K. Dransfeld, Phys. Rev. 117, 1245 (1960).

[17]R. Merlin, K. Bajema, R. Clarke, F. Y. Juang, and P. K. Bhattacharya, Phys. Rev. Lett. 55, 1768 (1985).

[18]V. Elser, Phys. Rev. B 32, 4892 (1985).

[19]R. K. P. Zia and W. J. Dallas, J. Phys. A 18, L341 (1985).

[20]V. Hoggatt, Fibonacci and Locas Numbers (Mifflin, Boston, 1969).
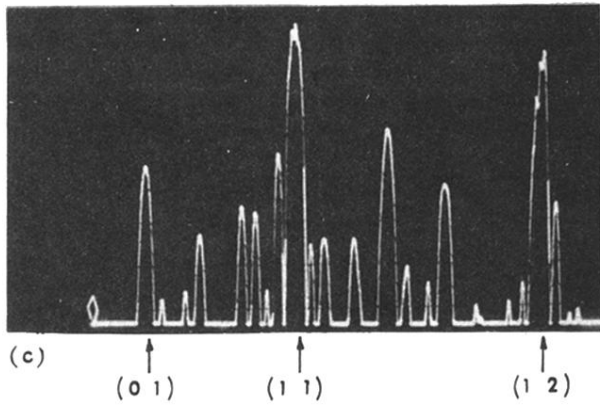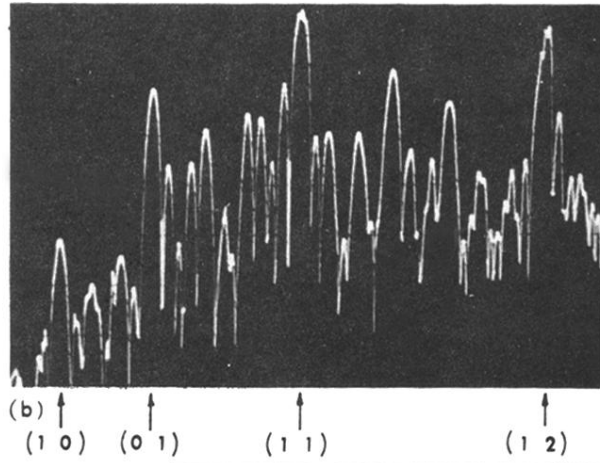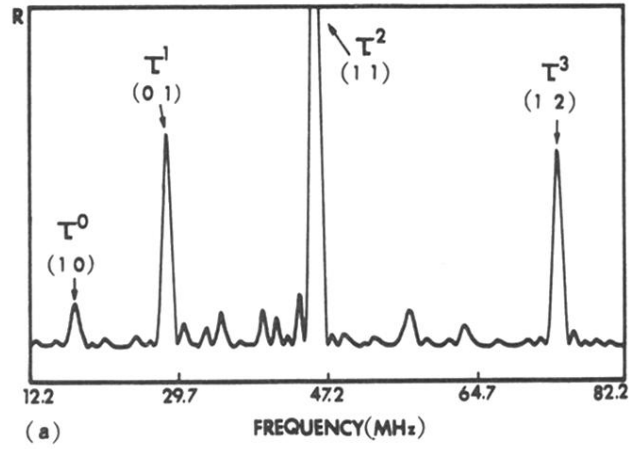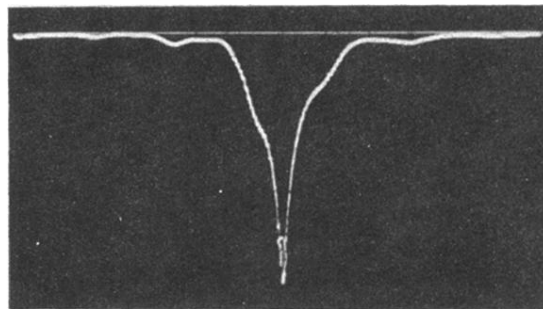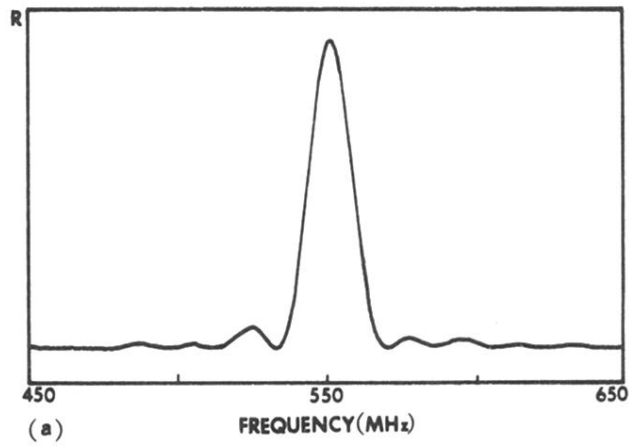
[21]H. R. Ma and C. H. Tsai, Phys. Rev. B 35, 9295 (1987).

FIG. 5. Ultrasonic spectrum for an eighth-generation Fibonacci acoustic superlattice. (a) Ultrasonic spectrum calculated for a $LiNbO_3$ crystal. $R$, relative value of radiation resistance. (b) Ultrasonic spectrum measured. (c) The same as (b) with the amplitude magnified. In both (b) and (c) the amplitude is in logarithmic scale.

FIG. 6. Ultrasonic spectrum for a periodic acoustic superlattice of a LiNbO$_3$ crystal. (a) Ultrasonic spectrum calculated. $R$, relative value of radiation resistance. (b) Measured magnitude of the reflection coefficient. The horizontal scale is frequency centered at 550 MHz with a scan width $f = 200$ MHz.